UC Riverside

UC Riverside Previously Published Works

Title

Prolonged activation of carbon dioxide-sensitive neurons in mosquitoes

Permalink

https://escholarship.org/uc/item/4b97b3qd

Journal

Interface Focus, 11(2)

ISSN

2042-8898

Authors

Chen, Stephanie Turner
Kowalewski, Joel
Ray, Anandasankar

Publication Date

2021-04-06

DOI

10.1098/rsfs.2020.0043

Peer reviewed

eScholarship.org Powered by the California Digital Library
University of California

INTERFACE FOCUS

royalsocietypublishing.org/journal/rsfs

Research

Cite this article: Chen ST, Kowalewski J, Ray A. 2021 Prolonged activation of carbon dioxide-sensitive neurons in mosquitoes. *Interface Focus* **11**: 20200043.
https://doi.org/10.1098/rsfs.2020.0043

Accepted: 9 December 2020

One contribution of 13 to a theme issue 'Carbon dioxide detection in biological systems'.

Subject Areas:
computational biology

Keywords:
CO_2, mosquito, olfaction, machine learning, electrophysiology

Author for correspondence:
Anandasankar Ray
e-mail: anand.ray@ucr.edu

†These authors contributed equally.

THE ROYAL SOCIETY PUBLISHING

Prolonged activation of carbon dioxide-sensitive neurons in mosquitoes

Stephanie Turner Chen[1,†], Joel Kowalewski[2,†] and Anandasankar Ray[1,2]

[1]Department of Molecular, Cell and Systems Biology, and [2]Interdepartmental Neuroscience Program, University of California, Riverside, CA 92521, USA

JK, 0000-0002-7060-7890; AR, 0000-0003-4133-2581

Many insects can detect carbon dioxide (CO_2) plumes using a conserved receptor made up of members of the gustatory receptor (Gr) family Gr1, Gr2 and Gr3. Mosquitoes are attracted to host animals for blood meals using plumes of CO_2 in the exhaled breath using the receptor expressed in the A neuron of the capitate peg sensilla type on the maxillary palps. The receptor is known to also detect several other classes of odorants, including ones emitted from human skin. Here, we discover that a common skin odorant, butyric acid, can cause a phasic activation followed by an unusually prolonged tonic activity after the stimulus is over in the CO_2 neurons of mosquitoes. The effect is conserved in both *Aedes aegypti* and *Anopheles gambiae* mosquitoes. This raises a question about its role in a mosquito's preference for the skin odour of different individuals. Butyric acid belongs to a small number of odorants known to cause the prolonged activation of the CO_2 receptor. A chemical informatic analysis identifies a specific set of physico-chemical features that can be used in a machine learning predictive model for the prolonged activators. Interestingly, this set is different from physico-chemical features selected for activators or inhibitors, indicating that each has a distinct structural basis. The structural understanding opens up an opportunity to find novel ligands to manipulate the CO_2 receptor and mosquito behaviour.

1. Introduction

Carbon dioxide (CO_2) serves as a long-distance orientation and host-seeking cue for most mosquito species. Human beings generate CO_2 odour plumes through exhaled breath, causing fluctuation in CO_2 between background (0.04%) and expired levels (4%). This intermittency in CO_2 concentration is thought to increase host-seeking behaviour in mosquitoes, causing them to fly upwind toward the odour source [1,2]. Once the mosquito has followed the CO_2 plume toward its source, it is thought that the insect will then detect other sensory cues such as skin odours and heat [3]. Not surprisingly, mosquito species, such as the ornithophilic *Culex quinquefasciatus* and the anthropophilic *Anopheles gambiae* and *Aedes aegypti*, are differentially attracted to host odours such as those from avian and human sources, respectively.

However, CO_2 is an emanation common to all hosts as it signifies the presence of a vertebrate's exhaled air. When presented in an optimal fashion, CO_2 can readily attract mosquitoes in the field and in the laboratory [4–7], as well as increase the sensitivity of mosquitoes to other human odours [2]. Since CO_2 is highly influential in host-seeking behaviour of many mosquito species, the majority of mosquito traps employ CO_2 as the primary lure. The maxillary palp is the CO_2 detecting organ, where of the three neurons housed in the club-shaped capitate peg (cp) sensilla, the cpA neuron expresses the CO_2 receptor Gr1, Gr2 and Gr3 (also called Gr22, Gr23 and Gr24) which belong to the gustatory receptor family [8,9]. These proteins are closely related to the CO_2 receptor of *Drosophila melanogaster*, Gr21a and Gr63a which are required for response to CO_2 [10,11].

© 2021 The Author(s) Published by the Royal Society. All rights reserved.

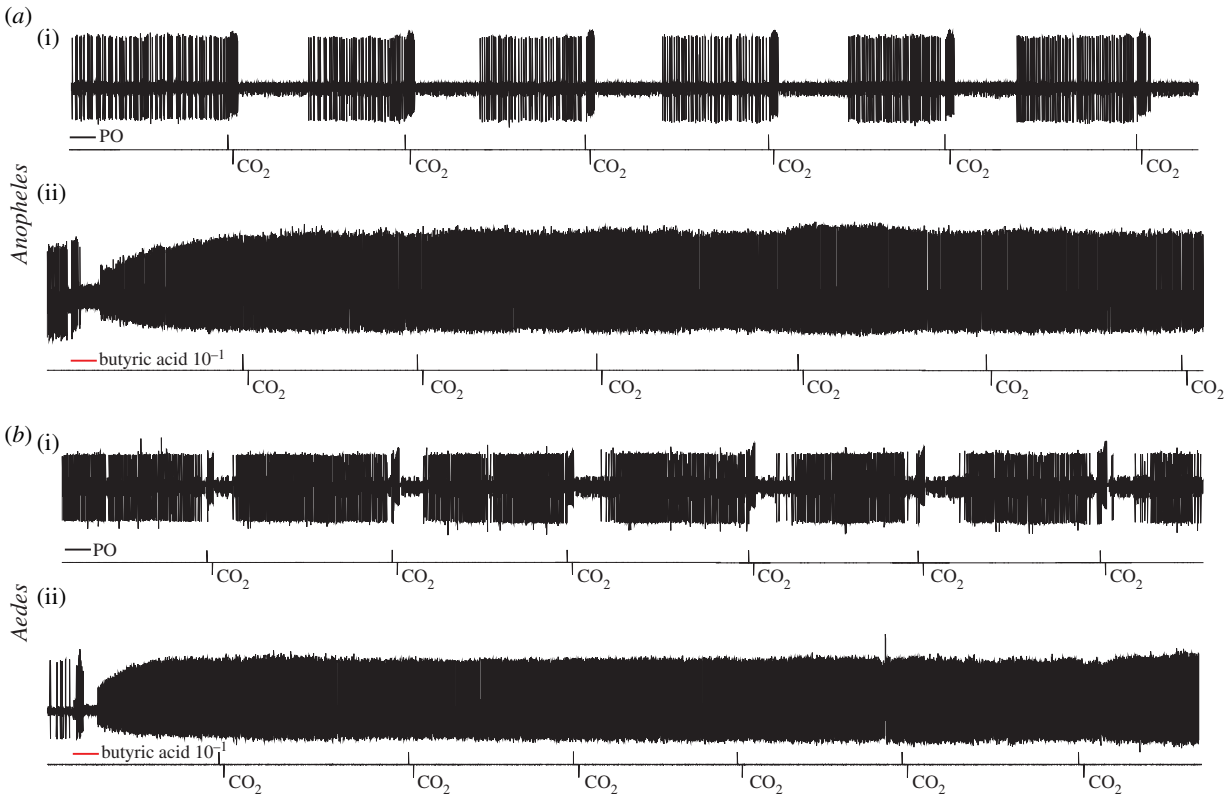

Figure 1. Butyric acid is an ultra-prolonged activator of the CO_2-sensitive neuron in *A. gambiae and A. aegypti*. Long-term traces from the cpA neuron of (*a*) *A. gambiae* and (*b*) *A. aegypti*. A 3 s stimulus paraffin oil (PO) (i) or butyric acid (ii) is given followed by 1 s pulses of 0.15% CO_2 every 30 s. Odour diluted 10^{-1}.

Apart from CO_2, this receptor is also activated and inhibited by an array of volatile odorants that can be grouped into multiple structural categories [12–16]. Each of the proteins in the receptor has a 7-transmembrane structure and while Gr2 and Gr3 constitute the core receptor, Gr1 increases sensitivity to CO_2 and to inhibitory odorants [17]. It has been previously shown that inhibition of the CO_2 response by volatile odorants corresponds to complete loss of innate CO_2 avoidance behaviour in *Drosophila* [13]. Given the reversal of behaviour to CO_2 in the presence of the inhibitory odorants, and that mosquito CO_2 receptors have high amino acid identity with the *Drosophila* ortholog Gr63a and Gr21a [8,10,18,19], we tested and identified similar odorants that could have a similar effect on CO_2-mediated host-seeking behaviour in mosquitoes [12–16]. The identified volatile odorants included: odours that inhibit the CO_2-sensitive neuron and are candidates for use in disruption of host-seeking behaviour, odours that activate the neuron and can be a substitute for CO_2 as a lure in trapping devices and odours that cause strong and prolonged activation of the CO_2 neuron which blocks the ability to detect changes in CO_2 concentration and therefore offers a novel approach for disruption of host-seeking. These compounds could be used as tools for mosquito control as they modify peripheral olfactory responses to one of the most important host-seeking cues. These odour-based strategies once developed could potentially lower the incidence of human–mosquito contact, and hence lower the spread of vector-borne diseases.

2. Results

In the past, we have used single-sensillum electrophysiology to screen a large number of odorants for their effect on the activity of the CO_2-sensitive neuron in the peg sensilla of the maxillary palp of female *A. gambiae*, *A. aegypti*, and *C. quinquefasciatus*. The cpA neuronal response to CO_2 is nearly identical in all three species and it can be unambiguously identified since it has a much larger spike amplitude than the other two neurons in the same sensillum. When looking for activator and inhibitory odorants, we also found that the responses showed significant conservation [12–16]. One of the interesting questions has been how volatile components of malodorous body odour might be interacting with the mosquito CO_2 receptor. Many of the malodorous compounds are due to bacterial breakdown of lipids, such as butyric acid. When performing the electrophysiological recording odour screens, we observed that butyric acid caused an initial phasic activation followed by inhibition of the CO_2 response (figure 1). However, following this brief phasic excitation and inhibition, the odorant induced a 'prolonged' tonic activation of the cpA neuron.

In previous studies, a prolonged tonic activity has been shown to mask the activation caused by subsequent exposures to CO_2 such as with 2,3-butanedione, (E)-2-methyl-but-2-enal, 3-methyl-2-butenal and 3-methylbutanal [12,15]. This type of effect has also been observed in other odorant receptor neurons with odorants like methyl 2-propenoate and methyl propionate [20]. To investigate if prolonged activation by butyric acid could also cause a reduced response to subsequent CO_2, *A. gambiae* and *A. aegypti* mosquitoes were exposed to a 3 s application of the odorant followed by repeated 1 s stimulus of 0.15% CO_2 applied every 30 s for a period of approximately 5 min. When comparing spike rate in both mosquito species, there is an increase in baseline activity of the cpA neuron (figures 1 and 2). However, the brief exposure to butyric acid significantly reduced CO_2

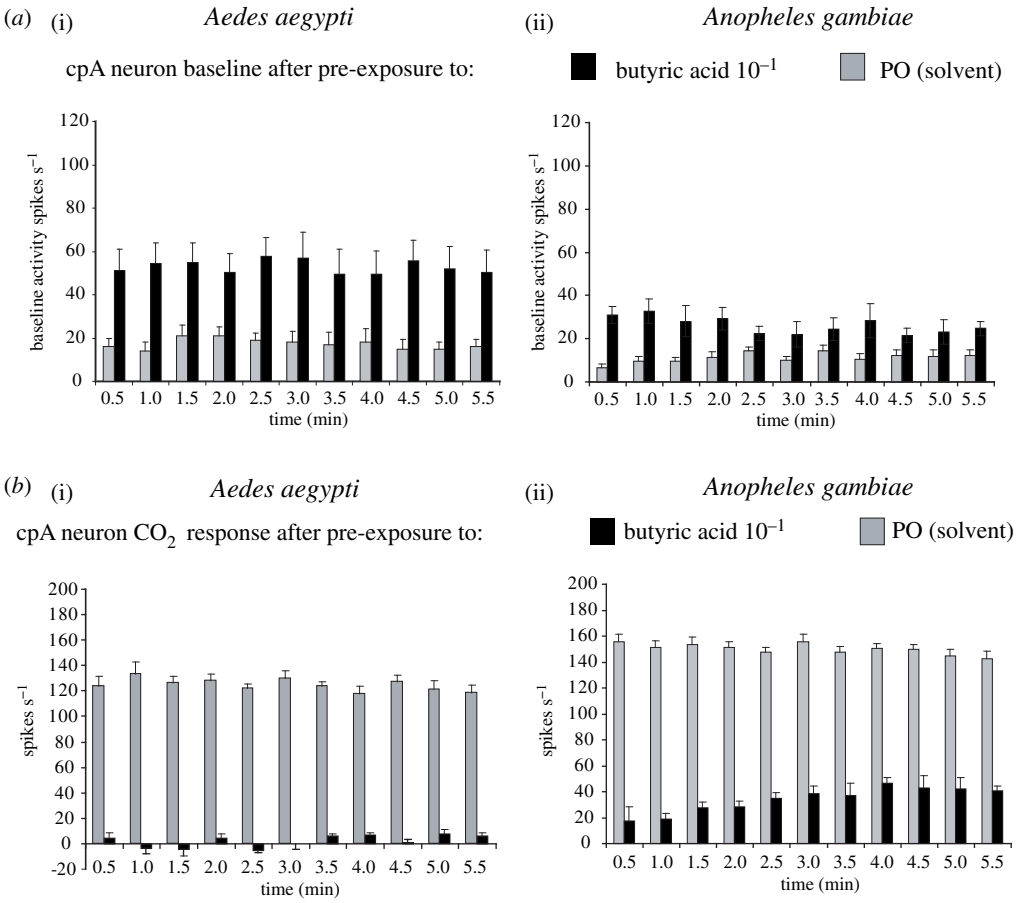

Figure 2. Butyric acid is an ultra-prolonged activator of the CO_2-sensitive neuron in *A. gambiae and A. aegypti*. (*a*) Mean baseline activity of the cpA neuron counted every 30 s interval after pre-exposure to a 3 s stimulus of butyric acid (10^{-1}) or paraffin oil (PO) solvent. (*b*) Mean change in frequency of response of the cpA neuron to stimulus of 1 s 0.15% CO_2 applied approximately every 30 s, following a 3 s pre-exposure to butyric acid (10^{-1}) or paraffin oil (PO) solvent. $n = 5$, error bars = s.e.m.

response for as long as 5.5 min in *A. gambiae* (figure 2ii), while the CO_2 response in *A. aegypti* was completely abolished (figure 2i). These results suggest that the prolonged tonic response can substantially impair the ability to sense other ligands like CO_2 for minutes.

To investigate the structural basis of the different activities, we first compared simple enriched substructures or cores among activators, prolonged activators and inhibitors of the cpA neuron (figure 3*a*). Interestingly, the correspondence between enriched substructures and activity was unclear. We next computed additional physico-chemical features, incorporating information about three-dimensional (3D) geometries, the distribution of charge across a molecule and other atomic-level properties describing bonds and bonding potential. As it is not feasible to manually search numerous features, we applied machine learning to identify sets of features that were particularly different among prolonged activators (figure 3*b*) and all other cpA activities. This approach involved iteratively training a support vector machine (SVM) on a portion of data, followed by predicting the remaining 'left out' portion (Methods). Consistent with the overlapping enriched substructures (figure 3*a*,*b*), the features that were predictive of prolonged activators often described 3D geometries (figure 3*c*). We next tested whether SVMs trained on these important features could successfully discriminate prolonged activators from the other cpA activities.

Receiver operating characteristic (ROC) analysis is a method for evaluating successful discrimination (see Methods). The machine learning model (SVM) predicts chemicals that were not in the training data. Predictions for these new chemicals are then compared to the ground truth. Success is defined by high positive (sensitivity) and low false-positive (1 − specificity) rates. Subsequently, an ROC plot shows the relationship between these two rates. The best possible performance is an area under the curve (AUC) of 1.0 (Methods). When we evaluated the model using this method, the high AUC suggested prolonged activators are physico-chemically distinct (figure 3*d*) (avg AUC = 0.958, shuffled activities, avg AUC = 0.592). But this is particularly true when considering physico-chemical properties (e.g. 3D geometries) other than enriched two-dimensional (2D) substructures or motifs, as indicated by the clear overlap in figure 3*a*.

3. Discussion

Interestingly, butyric acid is a component of human sweat [21], which has been shown to activate as well as inhibit several sensilla tricodae in *A. gambiae* [22,23]. Although human sweat is highly attractive to anthropophilic mosquitoes [24,25], it is not clear what role carboxylic acids play in the attractiveness of this host odour blend. For example, there are several conflicting studies as to the attractiveness of carboxylic acids to mosquitoes where in some cases carboxylic acids are actually unattractive [24,26,27]. The varied attractiveness to human skin odours could be attributed to intraspecific preferences for certain human hosts as their

(*a*)

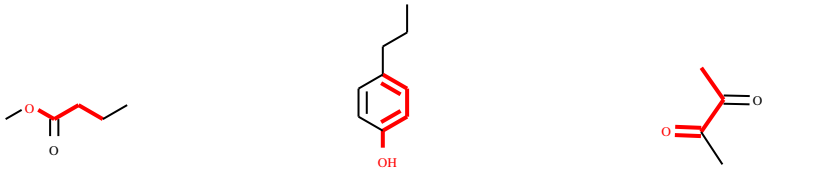

(*b*)

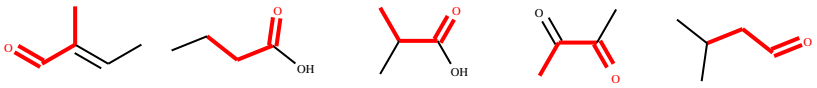

(*c*)

feature	description
CIC5	complementary information content index (neighbourhood symmetry of 5-order)
Eig03_AEA(dm)	eigenvalue n. 3 from augmented edge adjacency mat. weighted by dipole moment
Eig05_EA(dm)	eigenvalue n. 5 from edge adjacency mat. weighted by dipole moment
Eig05_EA(ed)	eigenvalue n. 5 from edge adjacency mat. weighted by edge degree
Eta_betaS_A	eta sigma average VEM coun
GATS2e	Geary autocorrelation of lag 2 weighted by Sanderson electronegativity
H-047	H attached to C1sp3, C0sp2
HATS4s	leverage-weighted autocorrelation of lag 4 / weighted by I-state
IC2	information content index (neighbourhood symmetry of 2-order)
MATS5i	Moran autocorrelation of lag 5 weighted by ionization potential
Mor03m	signal 03 / weighted by mass
Mor04m	signal 04 / weighted by mass
Mor07i	signal 07 / weighted by ionization potential
Mor15s	signal 15 / weighted by I-state
Mor20s	signal 20 / weighted by I-state
Psi_e_0d	electrotopological state pseudoconnectivity index - type 0d
Psi_e_1d	electrotopological state pseudoconnectivity index - type 1d
R2p	R autocorrelation of lag 2 / weighted by polarizability
R4e+	R maximal autocorrelation of lag 4 / weighted by Sanderson electronegativity
R4s+	R maximal autocorrelation of lag 4 / weighted by I-state
R5i+	R maximal autocorrelation of lag 5 / weighted by ionization potential
SHP2	average shape profile index of order 2
SpMax_B(s)	leading eigenvalue from Burden matrix weighted by I-state
SpMaxA_B(s)	normalized leading eigenvalue from Burden matrix weighted by I-state
SpMaxA_EA(ed)	normalized leading eigenvalue from edge adjacency mat. weighted by edge degree
X3A	average connectivity index of order 3
X5A	average connectivity index of order 5
X5Av	average valence connectivity index of order 5
Xindex	Balaban X index
Yindex	Balaban Y index

(*d*)

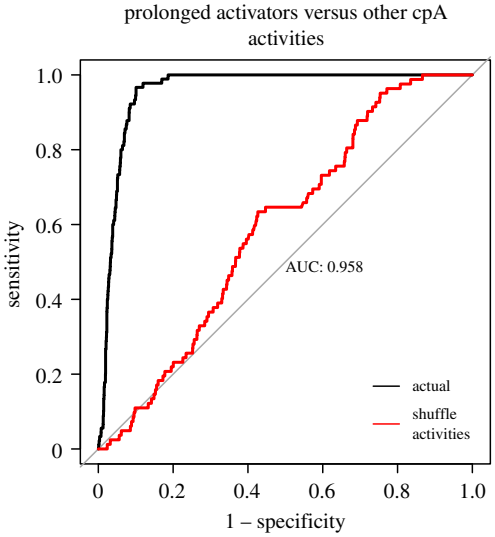

Figure 3. Ultra-prolonged activators of the CO_2 neuron have a shared substructure and can be modelled computationally. (*a*) Examples of cpA activators, inhibitors and prolonged activators, enriched substructures in red. The activators, inhibitors and prolonged activators have similar enriched substructures or simple 2D structural features. (*b*) Additional examples of the prolonged activators, enriched substructure in red. (*c*) Table of top 2D/3D chemical features to discriminate prolonged activators of cpA from the activators and inhibitors. (*d*) Support vector machines (SVM) are iteratively fit on a portion of chemicals, 'training', and then predictions are made for the chemicals excluded from training; the quality of the predictions is assessed using ROC analysis. The plot shows the performance across three SVM models trained with slightly different chemical feature combinations (black coloured curve). Random or chance level performance is estimated by training these SVM models on shuffled activity labels (red coloured curve). Diagonal line is the theoretical random performance (AUC = 0.50). The *y*-axis (sensitivity) is the true positive rate whereas the *x*-axis is the false-positive rate (1 — specificity). Each point along the curve is from computing these rates at different probability score cutoffs; the probability scores (0–1.0) are assigned by the SVM model to new chemicals. These scores are the predictions that a chemical is a prolonged activator of cpA. It is expected that high scores are assigned to prolonged activators and low scores to the other cpA activities. The ROC plot tests this expectation. Additional details included in Methods.

emanations differ from individual to individual [3,4,28–30]. No study, to our knowledge, has looked at the attractiveness of carboxylic acids (or human odours) as it pertains to activation or inhibition of neurons in the maxillary palp. It is unclear from these and other studies if behavioural responses observed result from a direct repellent effect or another mechanism whereby the insects are failing to respond to normally attractive cues such as CO_2. Perhaps levels of butyric acid from person to person can contribute to host preference in the mosquito as a means of CO_2 response modification. Future behavioural assays will be required to test this hypothesis.

Although the substructure that was enriched among the prolonged activators differed subtly from cpA activators and inhibitors, more rigorous 3D analyses indicated the presence of distinct physico-chemical attributes for each. When incorporating these features into a machine learning model, we observed high success rates for classifying prolonged activators from other cpA activities. The degree of success implies cpA prolonged activation is indeed related to a set of physico-chemical attributes, and machine learning could therefore play an important role in identifying new ligands. The prolonged activator represents an interesting class of ligand, though there are currently few examples. Machine

learning pipelines could predict new prolonged activators and help resolve even finer distinctions from cpA activators and inhibitors. This would subsequently have long-term implications for mosquito vector control strategies.

4. Methods

4.1. Mosquitoes

A. aegypti wild-type (Orlando strain) and *A. gambiae* (recently renamed *Anopheles coluzzii*) were maintained using standard protocols in an insectary at approximately 27°C, approximately 70–80% humidity on a 14 L : 10 D h photoperiod.

4.2. Electrophysiology

Extracellular single-unit recordings were performed as described previously [13] with few modifications. Chemicals were of the highest purity available, typically greater than 99% (Sigma-Aldrich). Odorants were diluted in paraffin oil at the indicated concentration. Unless indicated 50 l of diluted odorant is applied per cartridge, and each cartridge used for three stimuli. A controlled volume of air at 5 ml s^{-1} was puffed through the odour cartridge containing vapours and was delivered into a constant humidified airstream of 10 ml s^{-1} that flowed over the fly antenna. The odorant vapour present in the cartridge was thus diluted approximately threefold before being passed over the fly (each delivery cartridge was used no more than three times; 10^{-1} stimulus = approximately 0.43 µg equivalent from cartridge/application; 10^{-2} stimulus = approximately 0.043 µg equivalent from cartridge/application). CO_2 stimulus was pulsed through a separate delivery system that delivered controlled pulses using a PSM 8000 microinjector (variable 2.5 – 6.5 ml s^{-1}) into the same humidified airstream, from either a 1% or 5% tank of CO_2 (Airgas). The baseline constant humidified airstream (10 ml s^{-1}) was generated from a purified air tank (Airgas) and mixed with a constant controlled volume (5 ml s^{-1}) of filtered room air (approx. 0.035% CO_2). For delivery of binary mixtures of CO_2 with another odorant, we ensured a steady concentration of CO_2 to the fly preparation as described in detail in [13]. Unless mentioned, responses were quantified by subtraction of baseline activity immediately preceding stimulus application from activity during the stimulus. For each odorant that had a long-term effect on CO_2 response, each recording was obtained from a naive insect.

4.3. Chemical informatics

Chemicals were analysed for maximum common substructures using RDKit (Python) [31]. The algorithm performs an exhaustive search for enriched structural patterns over a set of chemicals. For larger, more diverse sets of chemicals specifying a threshold value can help the algorithm converge on more substantive structural patterns. Here, we set the threshold at 0.5, which ensures that half of the chemical set should contain the pattern. This algorithm was run separately for activators, inhibitors and prolonged activators of cpA. The distinction between the three (activators, inhibitors and prolonged activators) was based on the spikes per second calculation, where inhibitors reduce activity below the baseline firing rate and activators increase activity above this rate; the prolonged activators significantly above.

Chemical structures were converted into 3D optimized geometries using RDKit (Python) [31]. The 3D chemical information was then supplied to alvaDesc, which computes approximately 5300 physico-chemical features. We later removed the features with low variance, high correlations ($r = 0.85$) and imputed missing values using the median.

4.4. Selecting important chemical features

The reduced feature set was then run through the recursive feature elimination algorithm over 300 train/test partitions (e.g. 10-fold cross-validation, repeated 30 times). Here, the algorithm involves iteratively fitting a support vector machine (radial basis function kernel) with different chemical feature sets on the training portion, predicting what remains. Subsequently, the average performance across these different feature sets provides an estimate of the number of features that are needed for successful predictions. This analysis suggested between 20 and 50 features. The importance of each feature is from the AUC achieved independently. A feature rank is assigned at the end of the cross-validation iterations.

Machine learning algorithms for feature selection are from the caret [32] and kernlab [33] packages in the R programming language and similar to the way it has been used for ligand prediction of human odorant neurons [34].

4.5. Machine learning

After selecting the physico-chemical features that are important for the task, models are trained using these features, and predictions are made for chemicals that are not in the training set to evaluate whether learning has indeed occurred. Here, three SVM models are fit, sampling different physico-chemical features. The individual predictions (probability scores) are then averaged. Each SVM learns a decision boundary from the physico-chemical features at training. To validate, new chemicals are repeatedly projected into this space. The location of this new chemical relative to the decision boundary provides the prediction, which is compared to an observed value or label (e.g. ground truth).

In machine learning terminology, iteratively training models and predicting new chemicals is referred to as cross-validation. Dividing the data into 10 different training and testing sets refers to 10-fold cross-validation. Here, we repeated this process five times (e.g. repeated 10-fold cross-validation). By using more than one model, it is possible to diversify the training, gaining more coverage of the data, getting better estimates of the error, and ultimately, in most cases, producing more generalizable predictions. Implementations of the machine learning algorithms are from the caret [32] and kernlab [33] packages in the R programming language

4.6. Support vector machine

The SVM algorithm uses kernels to facilitate the learning of complex, nonlinear decision boundaries. The kernel is a function that projects the chemical data into a new space where non-obvious boundaries among chemicals of different classes are increasingly identifiable. The SVM implemented here used the Gaussian or radial basis function kernel. This kernel is adjusted during the training phase through the sigma parameter, which determines the influence of chemicals or data points that are far from the decision boundary. This affects the prediction of new chemicals and therefore the proper value is set by removing and predicting a small subset of chemicals while training. An additional parameter, C, defines the cost associated with incorrect prediction performance. As the cost increases, the boundary adapts to improve performance. However, setting the cost value too high produces irregular boundaries that fail to generalize to new chemicals or data points. The proper cost value is therefore set alongside sigma using the approach discussed above.

4.7. Receiver operating characteristic analysis

ROC analysis graphically represents classification success and/or failure by comparing the true positive (y-axis: sensitivity)

and false-positive rates (x-axis: 1-specificitiy). In this study, it is analysing the success or failure of a machine learning model to classify 'prolonged activators' versus other activities on the cpA neuron. The trained machine learning model takes the chemical features of a new chemical (e.g. not in the training data) as input. Then it assigns a probability score to this new chemical based on its similarity to the prolonged activators and other activities on cpA from the training data. Subsequently, the ROC analysis defines cutoffs or thresholds for these probability scores. For example, if the score is above 0.50, then these chemicals are labelled as prolonged activators or simply positive/active cases. The labels are compared to the observed cpA activity, yielding a tally of true positives and false positives that are converted into rates. In the ROC plot, this information is a single point (x, y). Continuing the above process for multiple cutoffs results in a curve. The success is evaluated as the area under the curve (AUC = 1.0; perfect success).

Typically, the curve is compared to a theoretical random classifier (AUC = 0.50), and this is shown as a diagonal that bisects the plot area. Because chance level performance depends on the classification problem, it may be higher or lower than AUC = 0.50. Some classification problems are, for instance, trivial, particularly if there are few positive and negative examples. The chance performance could match the performance of the actual machine learning model. To address this, we trained the models using shuffled data, while keeping other parameters constant. This showed that the success of the actual model(s) was not attributable to chance.

Data accessibility. Data used in the analyses are included in the figures and supplements. These data will also be provided in other formats if requested from the communicating author.

Authors' contributions. S.T.C. performed the electrophysiology experiments and helped write the first draft of the manuscript; J.K. performed the computational analyses and helped write the manuscript; A.R. supervised the project, obtained funding and wrote the manuscript with help from other authors.

Competing interests. J.K. and A.R. are listed as inventors in patent applications filed by UCR. A.R. is founder of Sensorygen Inc. that discovers novel insect repellents, flavours and fragrances.

Funding. The work was supported by grants RO1AI087785 (NIAID) and RO1DC014092 (NIDCD) to A.R. from the NIH, USA. The granting agencies had no role in experimental design or analysis.

Acknowledgements. We thank members of the laboratory for discussions.

References

1. Carde RT, Willis MA. 2008 Navigational strategies used by insects to find distant, wind-borne sources of odor. *J. Chem. Ecol.* **34**, 854–866. (doi:10.1007/s10886-008-9484-5)
2. Dekker T, Geier M, Carde RT. 2005 Carbon dioxide instantly sensitizes female yellow fever mosquitoes to human skin odours. *J. Exp. Biol.* **208**, 2963–2972. (doi:10.1242/jeb.01736)
3. Takken W, Knols BGJ. 1999 Odor-mediated behavior of Afrotropical malaria mosquitoes. *Annu. Rev. Entomol.* **44**, 131–157. (doi:10.1146/annurev.ento.44.1.131)
4. Dekker T, Takken W, Braks MAH. 2001 Innate preference for host-odor blends modulates degree of anthropophagy of Anopheles gambiae sensu lato (Diptera : Culicidae). *J. Med. Entomol.* **38**, 868–871. (doi:10.1603/0022-2585-38.6.868)
5. Cooperband MF, Carde RT. 2006 Orientation of Culex mosquitoes to carbon dioxide-baited traps: flight manoeuvres and trapping efficiency. *Med. Vet. Entomol.* **20**, 11–26. (doi:10.1111/j.1365-2915.2006.00613.x)
6. Xue RD, Doyle MA, Kline DL. 2008 Field evaluation of CDC and Mosquito Magnet (R) X traps baited with dry ice, CO_2 sachet, and octenol against mosquitoes. *J. Am. Mosq. Control Assoc.* **24**, 249–252. (doi:10.2987/5701.1)
7. Grant AJ, OConnell RJ. 1996 Electrophysiological responses from receptor neurons in mosquito maxillary palp sensilla. *Olfaction Mosq. Host Interact.* **200**, 233–253.
8. Lu T *et al.* 2007 Odor coding in the maxillary palp of the malaria vector mosquito Anopheles gambiae. *Curr. Biol.* **17**, 1533–1544. (doi:10.1016/j.cub.2007.07.062)
9. Syed Z, Leal WS. 2007 Maxillary palps are broad spectrum odorant detectors in Culex quinquefasciatus. *Chem. Senses* **32**, 727–738. (doi:10.1093/chemse/bjm040)
10. Robertson HM, Kent LB. 2009 Evolution of the gene lineage encoding the carbon dioxide receptor in insects. *J. Insect Sci.* **9**, 1–14. (doi:10.1673/031.009.1901)
11. Jones WD, Cayirlioglu P, Kadow IG, Vosshall LB. 2007 Two chemosensory receptors together mediate carbon dioxide detection in *Drosophila*. *Nature* **445**, 86–90. (doi:10.1038/nature05466)
12. Turner SL, Li N, Guda T, Githure J, Carde RT, Ray A. 2011 Ultra-prolonged activation of CO_2-sensing neurons disorients mosquitoes. *Nature* **474**, 87–91. (doi:10.1038/nature10081)
13. Turner SL, Ray A. 2009 Modification of CO_2 avoidance behaviour in *Drosophila* by inhibitory odorants. *Nature* **461**, 277–281. (doi:10.1038/nature08295)
14. Coutinho-Abreu IV, Sharma K, Cui L, Yan G, Ray A. 2019 Odorant ligands for the CO_2 receptor in two Anopheles vectors of malaria. *Sci. Rep.* **9**, 2549. (doi:10.1038/s41598-019-39099-0)
15. Tauxe GM, MacWilliam D, Boyle SM, Guda T, Ray A. 2013 Targeting a dual detector of skin and CO_2 to modify mosquito host seeking. *Cell* **155**, 1365–1379. (doi:10.1016/j.cell.2013.11.013)
16. MacWilliam D, Kowalewski J, Kumar A, Pontrello C, Ray A. 2018 Signaling mode of the broad-spectrum conserved CO_2 receptor is one of the important determinants of odor valence in *Drosophila*. *Neuron* **97**, 1153–1167 e4. (doi:10.1016/j.neuron.2018.01.028)
17. Kumar A, Tauxe GM, Perry S, Scott CA, Dahanukar A, Ray A. 2020 Contributions of the conserved insect carbon dioxide receptor subunits to odor detection. *Cell Rep.* **31**, 107510. (doi:10.1016/j.celrep.2020.03.074)
18. Kent LB, Walden KKO, Robertson HM. 2008 The Gr family of candidate gustatory and olfactory receptors in the yellow-fever mosquito Aedes aegypti. *Chem. Senses* **33**, 79–93. (doi:10.1093/chemse/bjm067)
19. Hill CA *et al.* 2002 G protein coupled receptors in Anopheles gambiae. *Science* **298**, 176–178. (doi:10.1126/science.1076196)
20. Boyle SM, McInally S, Tharadra S, Ray A. 2016 Short-term memory trace mediated by termination kinetics of olfactory receptor. *Sci. Rep.* **6**, 19863. (doi:10.1038/srep19863)
21. Cork A, Park KC. 1996 Identification of electrophysiologically-active compounds for the malaria mosquito, Anopheles gambiae, in human sweat extracts. *Med. Vet. Entomol.* **10**, 269–276. (doi:10.1111/j.1365-2915.1996.tb00742.x)
22. van den Broek IVF, den Otter CJ. 1999 Olfactory sensitivities of mosquitoes with different host preferences (Anopheles gambiae s.s., An. arabiensis, An. quadriannulatus, An. m. atroparvus) to synthetic host odours. *J. Insect. Physiol.* **45**, 1001–1010. (doi:10.1016/S0022-1910(99)00081-5)
23. Meijerink J, van Loon JJA. 1999 Sensitivities of antennal olfactory neurons of the malaria mosquito, Anopheles gambiae, to carboxylic acids. *J. Insect Physiol.* **45**, 365–373. (doi:10.1016/S0022-1910(98)00135-8)
24. Healy TP, Copland MJW, Cork A, Przyborowska A, Halket JM. 2002 Landing responses of Anopheles gambiae elicited by oxocarboxylic acids. *Med. Vet. Entomol.* **16**, 126–132. (doi:10.1046/j.1365-2915.2002.00353.x)
25. Braks MAH, Takken W. 1999 Incubated human sweat but not fresh sweat attracts the malaria mosquito Anopheles gambiae sensu stricto. *J. Chem. Ecol.* **25**, 663–672. (doi:10.1023/A:1020970307748)
26. Smallegange RC, Qiu YT, van Loon JJA, Takken W. 2005 Synergism between ammonia, lactic acid and carboxylic acids as kairomones in the host-seeking

behaviour of the malaria mosquito Anopheles gambiae sensu stricto (Diptera : Culicidae). *Chem. Senses* **30**, 145–152. (doi:10.1093/chemse/bji010)

27. Mboera LEG, Knols BGJ, Takken W, dellaTorre A. 1997 The response of Anopheles gambiae sl and A-funestus (Diptera: Culicidae) to tents baited with human odour or carbon dioxide in Tanzania. *Bull. Entomol. Res.* **87**, 173–178. (doi:10.1017/S0007485300027322)
28. Acree Jr F, Turner RB, Gouck HK, Beroza M, Smith N. 1968 L-lactic acid: a mosquito attractant isolated from humans. *Science* **161**, 1346–1347. (doi:10.1126/science.161.3848.1346)
29. Besansky NJ, Hill CA, Costantini C. 2004 No accounting for taste: host preference in malaria vectors. *Trends Parasitol.* **20**, 249–251. (doi:10.1016/j.pt.2004.03.007)
30. Qiu YT, Smallegange RC, Hoppe S, Loon J, Bakker E-J, Takken W. 2004 Behavioural and electrophysiological responses of the malaria mosquito Anopheles gambiae Giles sensu stricto (Diptera: Culicidae) to human skin emanations. *Med. Vet. Entomol.* **18**, 429–438. (doi:10.1111/j.0269-283X.2004.00534.x)
31. Landrum G. 2006 RDKit: open-source cheminformatics. See http://www.rdkit.org.
32. Kuhn M. 2008 caret package. *J. Stat. Softw.* **28**, 1–26. (doi:10.18637/jss.v028.i05)
33. Karatzoglou A, Smola A, Hornik K, Zeileis A. 2004 kernlab: an S4 package for kernel methods in R. *J. Stat. Softw.* **11**, 1–20. (doi:10.18637/jss.v011.i09)
34. Kowalewski J, Ray A. 2020 Predicting human olfactory perception from activities of odorant receptors. *iScience* **23**, 101361. (doi:10.1016/j.isci.2020.101361)